Comparison of Admission Perfusion Computed Tomography and Qualitative Diffusion- and Perfusion-Weighted Magnetic Resonance Imaging in Acute Stroke Patients

M. Wintermark, MD; M. Reichhart, MD; O. Cuisenaire, PhD; P. Maeder, MD; J.-P. Thiran, PhD; P. Schnyder, MD; J. Bogousslavsky, MD; R. Meuli, MD, PhD

Background and Purpose—Besides classic criteria, cerebral perfusion imaging could improve patient selection for thrombolytic therapy. The purpose of this study was to compare quantitative perfusion CT imaging and qualitative diffusion- and perfusion-weighted MRI (DWI and PWI) in acute stroke patients at the time of their emergency evaluation.

Methods—Thirteen acute stroke patients underwent perfusion CT and DWI or PWI on admission. The size of infarct and ischemic lesion (infarct plus penumbra) on the admission perfusion CT was compared with that of the MR abnormalities as shown on the DWI trace and on the relative cerebral blood volume, cerebral blood flow, time to peak, and mean transit time maps calculated from PWI studies.

Results—The most significant correlation was found between infarct size on the admission perfusion CT and abnormality size on the admission DWI map ($r=0.968$, $P<0.001$). A significant correlation was also observed between the size of the ischemic lesion (infarct plus penumbra) on the admission perfusion CT and the abnormality size on the mean transit time map calculated from admission PWI ($r=0.946$, $P<0.001$). Information about cerebral infarct and total ischemia (infarct plus penumbra) carried by both imaging techniques was similar, with slopes of 0.913 and 0.905, respectively.

Conclusions—An imaging technique may be helpful in the identification of cerebral penumbra in acute stroke patients and thus in the selection of patients for thrombolytic therapy. Perfusion CT and DWI/PWI are equivalent in this task. **(*Stroke*. 2002;33:2025-2031.)**

Key Words: cerebral ischemia ■ perfusion ■ tomography, x-ray computed ■ thrombolytic therapy

Strokes are the third-leading cause of death, after cardiovascular diseases and cancers. Each year, they are diagnosed in 750 000 patients and contribute to at least 150 000 deaths in the United States.[1,2] Although thrombolysis is now an approved therapy for acute human stroke,[3] many stroke patients do not benefit from such treatment. Others even are harmed by thrombolysis; it is responsible for up to 15% to 26% of cerebral hemorrhage.[4,5] Present indications for intravenous thrombolytic therapy depend on the time interval since the onset of symptoms (<3 hours) and noncontrast cerebral CT findings [absence of cerebral hemorrhage and a cerebral hypodensity extending to less than one third of the middle cerebral artery (MCA) territory].[1,6] Many investigators believe that the selection of patients for thrombolysis could be improved by evaluation of brain perfusion before thrombolysis, which seems to be linked to an unfavorable risk-to-benefit ratio in cases of extensive oligemia in the territory of an occluded MCA.[7–12] Because the aim of thrombolysis is to save the ischemic penumbra, ie, the region of decreased perfusion not situated below the critical level for maintenance of the Na^+,K^+-ATPase pump and thus potentially reversible,[13–17] the goal in using a cerebral perfusion imaging technique is to visualize the ischemic penumbra and hence to identify at an early stage the difference between undamaged and salvageable cerebral parenchyma on one hand and unsalvageable on the other. Thrombolysis performed on patients with extensive cerebral infarcts with limited penumbra not only may prove to be of little benefit but also may increase the risk of intracranial bleeding.[8,12,18]

Conventional T2-weighted images and CT studies are typically abnormal 6 to 18 hours after the onset of ischemia. On the other hand, diffusion- and perfusion-weighted MR imaging (DWI and PWI) examinations have been reported to provide an early measure of brain metabolic and hemodynamic insufficiency as soon as minutes to hours after onset.[7–9,19–26] Currently, many investigators hypothesize that the DWI abnormality represents the cerebral infarct, whereas PWI abnormalities that are not yet diffusion abnormal may

Received December 29, 2001; final revision received April 12, 2002; accepted April 26, 2002.

From the Departments of Diagnostic and Interventional Radiology (M.W., P.M., P.S., R.M.) and Neurology (M.R., J.B.), University Hospital, and Signal Processing Laboratory, Swiss Federal Institute of Technology (O.C., J.-P.T.), Lausanne, Switzerland.

Reprint requests to Max Wintermark, MD, Department of Diagnostic and Interventional Radiology, CHUV-BH07, 1011 Lausanne, Switzerland. E-mail Max.Wintermark@chuv.hospvd.ch

Stroke **is available at http://www.strokeaha.org** **DOI: 10.1161/01.STR.0000023579.61630.AC**

stand for penumbra.[7–9,19,27,28] This DWI-PWI mismatch at early time points corresponds to a subsequent enlargement of the lesion volume.[26,28–31] DWI and PWI can thus improve the selection of patients with potentially favorable outcome in case of acute ischemic stroke.[7–9,19,30–33]

Perfusion CT is another imaging technique proposed for evaluating acute stroke patients at the time of their emergency evaluation. Perfusion CT is a modern imaging technique that can be performed on acute stroke patients. It involves the sequential acquisition of cerebral CT images performed in cine mode during the intravenous administration of iodinated contrast material. Perfusion CT has been reported to allow accurate quantitative assessment of cerebral blood flow (CBF) and cerebral blood volume (CBV).[34] It also allows delineation of cerebral infarct and cerebral tissue at risk for inclusion into the final infarct according to a method validated by comparison with delayed MR.[35]

In this study, we prospectively evaluated acute stroke patients by using both perfusion CT and DWI and PWI. Our purpose was to compare and correlate the various parameters characterizing brain perfusion that can be taken from perfusion CT and MR studies.

Materials and Methods

Patients

Our series consisted of 13 consecutive acute stroke adult patients (9 men, 4 women; median age, 68 years; interquartile range, 61 to 75 years). These patients were prospectively identified in the Emergency Department of our institution from March 2000 to June 2001. Inclusion criteria included acute ischemic stroke diagnosed on the basis of clinical and noncontrast CT data and both CT and MR examinations performed ≤3 hours after symptom onset. Exclusion criteria included potential treatment delay consecutive to performing MR examination, as well as contraindications to iodinated contrast material administration or to MRI. Patient characteristics, noncontrast CT findings, and location of the DWI abnormality are summarized in Table 1.

In all 13 patients, noncontrast baseline cerebral CT was immediately followed by perfusion CT, which is included in the initial routine survey of acute stroke patients at our institution. All 13 patients also underwent a cerebral and cervical CT-angiography.

MR examination, including sagittal T1-weighted, axial T2-weighted, axial DWI and PWI series, as well as cerebral and cervical MR-angiography, was performed in all 13 patients immediately after the CT survey. The time intervals from symptom onset to admission to the emergency room, perfusion CT, and MR were recorded. The permeability of intracranial and extracranial cerebral vessels was assessed from the CT-angiography, MR-angiography, and PWI.

This study protocol was approved by our review board, and institutional informed-consent guidelines were followed.

Imaging Techniques

The perfusion CT examination consisted of two 40-second series at an interval of 5 minutes, each series consisting of 1 image per second in cine mode during intravenous administration of iodinated contrast material. The acquisition parameters for both series were 80 kilovolt (peak; kVp) and 100 mA.[36] For each series, CT scanning was initiated 7 seconds after injection of 50 mL iohexol (300 mg/mL iodine, Accupaque 300, Nycomed) at a rate of 5 mL/s into an antecubital vein with a power injector (CT9000, Libel-Flarsheim Co). The time delay before contrast material reached the brain parenchyma allowed baseline images without contrast enhancement to be acquired. Waiting 5 minutes between the 2 perfusion CT series allows a substantial lowering of iodinated contrast material blood concentration after the first intravenous administration of iodinated contrast material and a restitution of baseline. Thus, realization of the second perfusion CT series is not affected by the first intravenous administration of iodinated contrast material.

TABLE 1. Characteristics of the 13 Acute Stroke Patients Who Underwent Both Perfusion CT and DWI or PWI at the Time of Emergency Evaluation

Patient	Age, y	Sex	Noncontrast CT Findings	Location of DWI Abnormality
1	51	F	Normal	Superficial left MCA
2	64	M	Normal	Right MCA
3*	71	M	Insula ribbon sign	Superficial left MCA
4	82	F	Insula ribbon sign	Left MCA and PCA
5†	71	M	Hypodensity and insula ribbon sign	Superficial left MCA
6	47	F	Normal	Right MCA
7	61	M	Insula ribbon sign	Superficial right MCA
8	61	M	Normal	Right MCA
9	50	M	Hypodensity, basal nuclei obscuration, and insula ribbon sign	Left MCA
10	79	F	Normal	Left MCA
11	68	M	Hypodensity and insula ribbon sign	Superficial left MCA
12	77	M	Normal	Left MCA
13	75	M	Hypodensity, insula ribbon sign, and hyperdense MCA	Right MCA

PCA indicates posterior cerebral artery.
*See Figure 1.
†See Figure 2.

Multidetector-array technology (Lightspeed CT unit, General Electric) allowed data acquisition from 2 adjacent 10-mm sections for each series. The 2 perfusion CT series thus allowed data acquisition in 4 adjacent 10-mm cerebral CT sections. The 4 studied cerebral sections were selected above the orbits to protect the lenses, running through the basal nuclei and then toward the vertex. They were identical to 4 among the 10-mm-thick noncontrast CT slices.

The cerebral and cervical CT-angiography was performed with the following parameters: 120 kVp; 240 mA; slice thickness, 2.5 mm; slice acquisition interval, 2 mm; pitch, 1.5:1; intravenous administration, 50 mL iodinated contrast material at 3 mL/s; and acquisition delay, of 10 seconds. Data acquisition was performed from the origin of the aortic arch branch vessels to the circle of Willis.

The MR examination was performed with a 1.5-T MR unit (Symphony MR unit, Siemens). It included DWI series: echoplanar single shot spin echo; repetition time (TR), 5000 ms; echo time (TE), 100 ms; b=0, 500, and 1000; twenty 5-mm-thick slices with a 1.5-mm gap; and matrix size, 128×128. PWI series was performed immediately afterward: echoplanar gradient echo; TR, 120 ms; TE, 45 ms; eleven 5-mm-thick slices with a 1.5-mm gap; matrix size, 128×128; and 50 acquisitions obtained every 1.32 seconds during intravenous administration of 0.2 mmol/kg Gd-DTPA (Omniscan, Nycomed Amersham), followed by a 15-mL saline flush at a rate of 5 mL/s into an antecubital vein with a power injector (Spectris MR Injection System, Medrad). T2*-weighted gradient-echo imaging technique rather than T2-weighted spin-echo echoplanar imaging technique was performed as required by the clinical trials in which the 13 patients were involved. For cerebral and cervical vessels, MR-angiography was performed using a time-of-flight multislab 3-dimensional fast low-angle shot technique. For cervical vessels, a 3-dimensional fast imaging with steady-state precession technique was also used during intravenous administration of a gadolinium bolus.

Data Processing

Perfusion CT data consist of time–contrast enhancement curves registered in each pixel, with the curves linearly related to the time-concentration curves for the iodinated contrast material. The perfusion CT data were analyzed by use of a homemade perfusion CT software (demonstrated at Radiological Society of North America, Chicago, Ill, 2001, and European Congress of Radiology, Vienna, Austria, 2002), the results of which have been validated by comparison with stable xenon CT.[34] This software relies on the central volume principle, which is the most accurate for low injection rates of iodinated contrast material.[37] The central volume principle uses a mathematical operation called deconvolution (least-mean-square deconvolution for the software used) to calculate a related mean transit time (MTT).[38–40] The deconvolution operation requires a reference arterial input function, the selection of which is automatically performed by the perfusion CT software used in a region of interest drawn by the user. Considering that all our patients were MCA stroke patients, time-concentration curves in each cerebral hemisphere have been deconvoluted by ipsilateral sylvian arterial input functions. The CBV map is inferred from a quantitative measurement of the partial size–averaging effect, which is absent at the center of the large superior sagittal venous sinus.[41–43] Finally, a simple equation combining CBV and MTT values leads to the CBF value[38–40]: CBF=(CBV/MTT). The perfusion CT results were then used to calculate the penumbra and infarct maps according to a previously reported method.[35] This method relies on the reported CBF threshold of ischemia and the preserved (penumbra) or the altered (infarct) autoregulatory processes. Thus, in this method, an ischemic cerebral area (penumbra plus infarct) was defined as including cerebral pixels with a CBF decrease of >34% compared with the corresponding region in the cerebral hemisphere defined as healthy on the basis of clinical symptoms. Within this selected area, pixels with CBV values higher or lower than 2.5 mL/100 g were selected as indicative of penumbra and infarct, respectively. The resulting cerebral infarct and penumbra maps were combined and graphically displayed as a prognostic map, with the penumbra in green and the infarct in red (Figures 1 and 2). The regional CBF and regional CBV thresholds of 34% and 2.5 mL/100 g were chosen in agreement with the values most frequently reported in the literature.[15,44–47] Such thresholding, combined with adequate spatial filtering, allows accurate infarct and penumbra maps, as demonstrated by comparison with delayed DWI.[35]

The PWI data were analyzed with perfusion analysis software (Functool, General Electric) and adequate postprocessing to create parametric maps of relative CBF, CBV, MTT, and time to peak (TTP), which designates the time to the peak signal change after the bolus is injected. Analysis of PWI data relies on principles similar to those applied to perfusion CT data but with some distinctions. Two are particularly relevant in the present setting. First, time-intensity curves in PWI are not linearly but logarithmically related to time-concentration curves.[48] Second, because of the susceptibility properties that underlie PWI, the reference arterial input cannot be selected within an arterial lumen, but only in the neighborhood of an artery.[48–50] This results in only qualitative or semiquantitative PWI results (whereas perfusion CT results are quantitative[34]) for a variety of reasons[44] that are still a matter of debate and are beyond the scope of this article. This also explains why we decided to use a planimetric method in the calculations rather than a numeric threshold method for determining the size of PWI abnormalities. Similar to what was described in by Sorenson et al,[8] 2 neuroradiologists who were blinded to each other were asked to determine the volume of abnormal signal for each of the PWI maps. The average of the 2 neuroradiologists' measurements was chosen as the reference for MR studies. This method more closely simulates how PWI maps are used in clinical practice.

Regarding DWI studies, abnormality size was measured on trace-weighted images, which allow clear delineation of the abnormal region because of the absence of interfering contrast between normal gray and white matter. Average diffusion coefficient maps were calculated and used to confirm that the trace abnormalities were hyperacute.

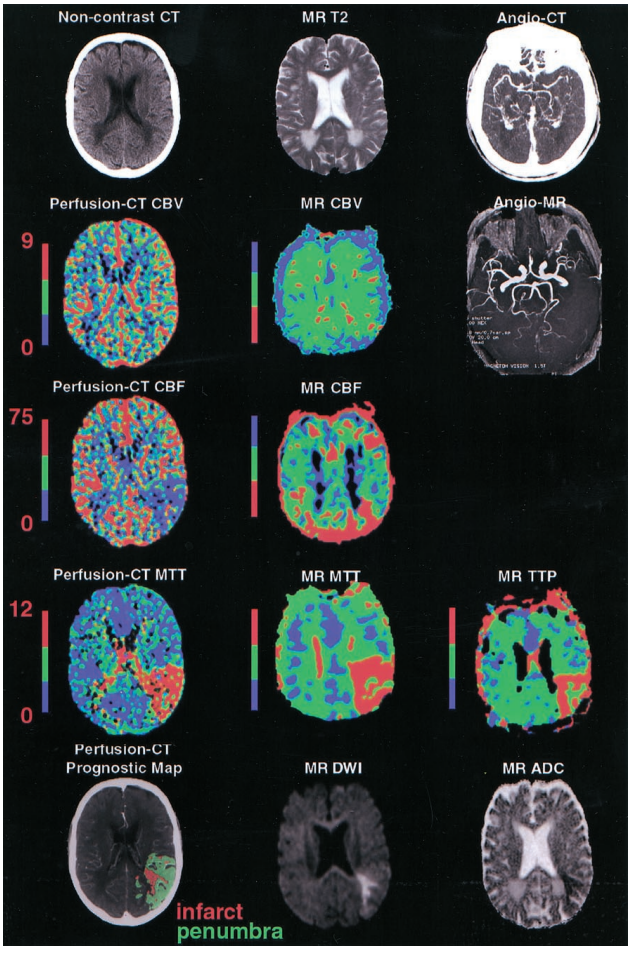

Figure 1. A 71-year-old male patient with sudden onset of a right face-arm-leg motor hemisyndrome associated with fluent aphasia 1.5 hours before admission. Noncontrast cerebral CT and perfusion CT were obtained 1.75 hours after symptom onset, whereas DWI or PWI was performed 20 minutes after CT. Noncontrast cerebral CT showed left insula ribbon sign. Sizes of cerebral infarct and CBV abnormality on perfusion CT (mL/100 g) is similar to that of DWI abnormality, whereas MR CBV map is unremarkable. Sizes of cerebral ischemic lesion and CBF/MTT abnormality on perfusion CT [(mL · 100 g^{-1} · min^{-1})/s] correlate with that of MR MTT abnormality (red) located on the left temporoparietal region, whereas they are larger than those of MR CBF and TTP abnormalities (red). CT-angiography and MR-angiography demonstrate occlusion of the left M1-M2 junction. This patient underwent successful thrombolysis with significant regression of symptoms.

Data Analysis

Six 5-mm-thick cerebral sections (with 1.5-mm gaps) in the DWI and PWI sequences were selected to constitute the volume corresponding most closely to that defined by the 4 adjacent 10-mm-thick noncontrast CT and perfusion CT sections. For each patient, the volumes (in milliliters) on corresponding noncontrast CT, perfusion CT, and DWI or PWI maps were compared through linear regression analysis with calculation of Pearson's linear correlation coefficients. Values of $P<0.001$ were considered statistically significant.

Results

Time Delays

The median time from symptom onset to emergency room admission was 1.5 hours (interquartile range, 1.3 to 2.0

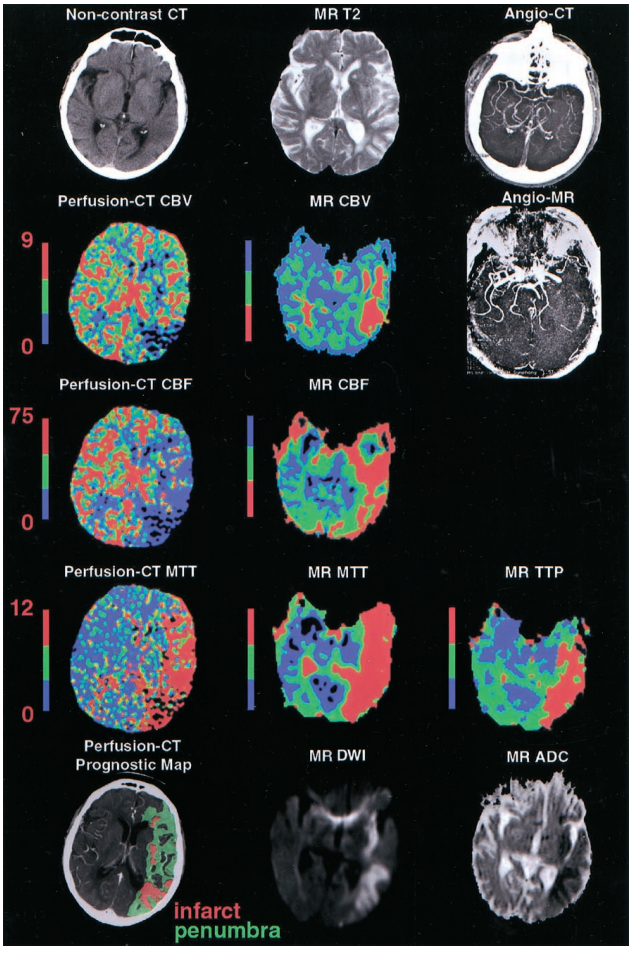

Figure 2. A 71-year-old male patient with sudden onset of a right face-arm-leg hemisyndrome associated with nonfluent aphasia. Noncontrast cerebral CT/perfusion CT and DWI or PWI were performed 2 and 2.3 hours after symptom onset, respectively. Noncontrast cerebral CT demonstrates left insula ribbon sign and left parietal hypodensity. MR CBV map is normal. Cerebral infarct and CBV abnormality on perfusion CT (mL/100 g) show sizes similar to that of DWI abnormality. Cerebral ischemic lesion and CBF MTT abnormality on perfusion CT [(mL · 100 g^{-1} · min^{-1})/s] and MR MTT abnormality (red) involve the whole left MCA territory, relating to an M1 occlusion on both CT-angiography and MR-angiography. This patient underwent unsuccessful thrombolysis.

hours); the median time from symptom onset to perfusion CT scanning was 2.0 hours (interquartile range, 2.0 to 2.8 hours). The median time to MR examination was 2.5 hours (interquartile range, 2.5 to 3.0 hours). Of the 13 patients, 9 underwent intravenous thrombolytic therapy. Thrombolysis was begun 2.8 hours (interquartile range, 2.5 to 2.8 hours) after symptom onset. No complications, in particular no hemorrhages, occurred in the 9 thrombolyzed patients.

Arterial Recanalization or Persistent Arterial Occlusion

In all 13 patients, admission CT-angiography demonstrated an occluded cerebral artery. In all of them, this cerebral arterial occlusion persisted on the MR-angiography and on PWI sequences.

Correlation Between Perfusion CT and DWI or PWI Results

The median size of cerebral hypodensity on noncontrast CT amounted to 0 mL (interquartile range, 0 to 4 mL). The median sizes of infarct and penumbra on perfusion CT were 19 and 120 mL (interquartile ranges, 14 to 44 and 80 to 140 mL, respectively). The median sizes of CBV, DWI, CBF, TTP, and MTT abnormalities amounted to 13, 21, 58, 96, and 129 mL (12 to 29, 14 to 42, 34 to 67, 58 to 125, and 98 to 168 mL), respectively.

The results of the linear regression analysis are summarized in Table 2 and are as follows. The size of CT hypodensity underestimates that of abnormalities on all perfusion CT and DWI or PWI maps (slopes <1). The perfusion CT infarct is larger than the MR CBV abnormality (slope >1), approximately equal to the DWI abnormality (slope almost unity), and smaller than the MR CBF, TTP, and MTT abnormalities. The correlation coefficient is the highest ($r=0.968$) and the probability values are the smallest ($P<0.001$) between the size of perfusion CT infarct and that of the DWI abnormality (Figure 3).

The perfusion CT ischemia (infarct plus penumbra) is larger than the MR CBV, DWI, CBF, and TTP abnormalities (slope >1) and approximately equal to the MR MTT abnormality (slope almost unity). The correlation coefficient is the highest ($r=0.946$) and the probability values are the smallest ($P<0.001$) between the size of perfusion CT ischemia and that of MR MTT abnormality (Figure 4). These results are illustrated in Figures 1 and 2.

Discussion

Only 13 patients could be enrolled in this study over 16 months. This limited number related mainly to the difficulty in obtaining MR examinations in the acute phase. Indeed, in our institution as in many others, MRI remains of limited availability in emergency settings because of overcrowded MR units and the absence of an MR scanner devoted to stroke patients.

On the other hand, perfusion CT can be easily achieved because it can be included in the cerebral CT survey undergone by almost every stroke patient.[35,51–53] Such CT survey, including noncontrast CT, 2 perfusion CT series, and CT-angiography, can be performed in <10 minutes. Perfusion CT is well tolerated by patients, even in the acute phase of stroke.[35,51–53]

The purpose of this study was to compare admission perfusion CT and admission DWI and PWI results. This comparison was allowed by the short time interval (median interval, 30 minutes) and by the absence of arterial recanalization between both examinations.

Our results outline a strong correlation between the size of cerebral infarct on perfusion CT and that of DWI abnormality ($r=0.968$), with a slope close to unity. The perfusion CT cerebral infarct is thus in agreement with the current opinion that DWI abnormality is unlikely to reverse and hence most likely correlates with the final infarct volume.[54] On the other hand, the size of the MR CBV abnormality underestimates both the sizes of cerebral infarct on perfusion CT and that of DWI abnormality (slope$=1.229$), even if these sizes are

TABLE 2. Comparison Between Abnormality Sizes on Perfusion CT and DWI or PWI

	y Axis								
	CT Hypodensity			Perfusion CT Infarct			Perfusion CT Ischemia (Infarct Plus Penumbra)		
x-Axis	Slope	*r*	*P*	Slope	*r*	*P*	Slope	*r*	*P*
MR CBV abnormality	0.479	0.419	0.195	1.229	0.948	0.007	1.572	0.685	0.059
DWI abnormality	0.425	0.671	0.223	0.913	0.968	<0.001	1.415	0.342	0.410
MR CBF abnormality	0.270	0.541	0.110	0.656	0.682	0.011	1.242	0.706	0.055
MR TTP abnormality	0.199	0.270	0.421	0.752	0.674	0.033	1.184	0.665	0.025
MR MTT abnormality	0.291	0.436	0.190	0.669	0.663	0.026	0.905	0.946	<0.001

significantly correlated ($r=0.948$). The underestimation of the size of the MR CBV abnormality induces in turn an underestimation of the size of the MR CBF abnormality because the latter proves equal to the CBV-to-MTT ratio.

Cerebral parenchyma with PWI abnormalities that do not yet show as ischemic on DWI has been postulated to represent penumbra.[26,28–31] PWI abnormalities can be characterized by different parameters. Among them, MTT is an easy-to-interpret parameter that is homogeneous in normal areas, allowing easy identification of abnormal hemodynamics.[29,30] A strong correlation was identified between the size of the MR MTT abnormality and the size of what is described by perfusion CT as cerebral tissue at risk for inclusion into the final infarct ($r=0.946$). This result is in agreement with previous reports demonstrating deconvolution methods as the most accurate in PWI result analysis.[55]

On the other hand, the size of the MR TTP abnormality underestimates the size of cerebral ischemia on perfusion CT and the size of the MR MTT abnormality. The TTP map describes changes in the arrival timing of blood to the ischemic area rather than decreased perfusion and is thus affected by parent vessel stenosis. TTP abnormalities do not necessarily reflect the severity of the perfusion deficit.[9]

Finally, the size of hypodensity on noncontrast cerebral CT underestimates that of all perfusion CT, DWI, and PWI abnormalities, which is in agreement with the fact that CT studies become typically abnormal only 6 to 18 hours after the onset of ischemia.

As described in Materials and Methods, brain coverage with perfusion CT was limited to a 40-mm thickness, whereas the whole brain can be assessed with DWI or PWI. As reported in Table 1, all 13 patients included in the present study were MCA stroke patients. In 0 of these 13 patients, the abnormalities seen on DWI or PWI examinations were located completely outside the 40-mm thickness covered by perfusion CT. In fact, the major portion of the cerebral ischemic area could be evaluated by perfusion CT. However, such a condition could occur, and limited coverage constitutes a limitation of perfusion CT technique, even if technological improvements in the near future will overcome this obstacle.

Finally, our cerebral CT survey protocol in stroke patients involves a total amount of 150 mL iodinated contrast material, which is rather high. Some concern may be raised about potential toxicity of iodinated contrast material on ischemic brain. In the present series, we never observed any deterioration in neurological condition after intravenous administration of iodinated contrast material. Cerebral digital subtracted angiography involves comparable volumes of iodinated contrast material but with a much higher blood concentration because of intra-arterial administration. Angiography, however, is often resorted to in the setting of strokes and remains a gold standard for stroke treatment. Finally, intravenous administration of nonionic iodinated contrast material has been demonstrated to be safe for ischemic cerebral parenchyma in animals.[56]

In conclusion, perfusion CT is an imaging technique that allows delineation of cerebral infarct and cerebral tissue at

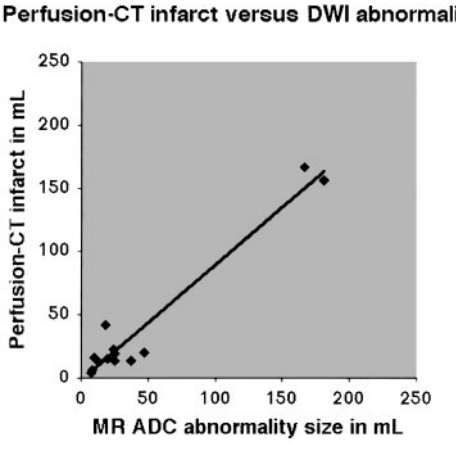

Figure 3. Significant correlation between the sizes of perfusion CT infarct and DWI abnormality (slope=0.913, $r=0.968$, $P<0.001$).

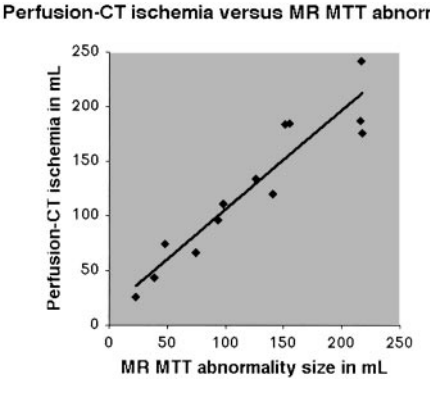

Figure 4. Significant correlation between the sizes of perfusion CT ischemia (infarct plus penumbra) and MR MTT abnormality (slope=0.905, $r=0.946$, $P<0.001$).

risk for inclusion into the final infarct, which are strongly correlated with DWI and PWI (MTT) MR results. The advantages of perfusion CT compared with DWI or PWI are related to its accessibility and its feasibility in acute stroke patients, as well as to the rapidity of data acquisition. Perfusion CT can be easily included in patients' imaging surveys at the time of their emergency evaluation. Brain coverage, however, remains more limited with perfusion CT than with DWI or PWI, and iodinated contrast material administration is required, although no toxicity of the latter could be observed.

Acknowledgments

We wish to acknowledge the skillful assistance of S. Behzad, chief MR technologist in the Department of Diagnostic and Interventional Radiology. We thank M. Rousselle for her help in editing the manuscript.

References

1. National Institute of Neurological Disorders and Stroke (NINDS) rt-PA Stroke Study Group. Tissue plasminogen activator for acute ischaemic stroke. *N Engl J Med*. 1995;33:1581–1587.
2. American Heart Association. *Stroke Facts*. Dallas, Tex: American Heart Association; 1999.
3. Hennerici M. Improving the outcome of acute stroke management. *Hosp Med*. 1999;60:44–49.
4. Zaheer A, Ozsunar Y, Schaefer PW. Magnetic resonance imaging of cerebral hemorrhagic stroke. *Top Magn Reson Imaging*. 2000;11: 288–299.
5. Mayer TE, Schulte-Altedorneburg G, Droste DW, Brückmann H. Serial CT and MRI of ischaemic cerebral infarcts: frequency and clinical impact of haemorrhagic transformation. *Neuroradiology*. 2000;42:233–239.
6. Hacke W, Kaste M, Fieschi C. Randomised double-blind trial placebo-controlled trial of thrombolytic therapy with intravenous therapy with intravenous alteplase in acute ischaemic stroke (ECASS II). *Lancet*. 1998;352:1245–1251.
7. Oppenheim C, Samson Y, Manai R, Lalam T, Vandamme X, Crozier S, Srour A, Cornu P, Dormont D, Rancurel G, Marsault C. Prediction of malignant middle cerebral artery infarction by diffusion-weighted imaging. *Stroke*. 2000;31:2175–2185.
8. Sorensen AG, Copen WA, Ostergaard L, Buonanno FS, Gonzalez RG, Rordorf G, Rosen BR, Schwamm LH, Weisskoff RM, Koroshetz WJ. Hyperacute stroke: simultaneous measurement of relative cerebral blood volume, relative cerebral blood flow, and mean tissue transit time. *Radiology*. 1999;210:519–527.
9. Beaulieu C, de Crespigny A, Tong DC, Moseley ME, Albers GW, Marks MP. Longitudinal magnetic resonance imaging study of perfusion and diffusion in stroke: evolution of lesion volume and correlation with clinical outcome. *Ann Neurol*. 1999;46:568–578.
10. Rubin G, Firlik AD, Levy EI, Pindzola RR, Yonas H. Relationship between cerebral blood flow and clinical outcome in acute stroke. *Cerebrovasc Dis*. 2000;10:298–306.
11. Karonen JO, Nuutinen J, Kuikka JT, Vanninen EJ, Vanninen RL, Partanen PL, Vainio PA, Roivainen R, Sivenius J, Aronen HJ. Combined SPECT and diffusion-weighted MRI as predictor of infarct growth in acute ischemic stroke. *J Nucl Med*. 2000;41:788–794.
12. Ezura M, Takahashi A, Yoshimoto T. Evaluation of regional cerebral blood flow using single photon emission tomography for the selection of patients for local fibrinolytic therapy of acute cerebral embolism. *Neurosurg Rev*. 1996;19:231–236.
13. Heiss WD, Grond M, Thiel A, von Stockhausen HM, Rudolf J. Ischemic brain tissue salvaged from infarction with alteplase. *Lancet*. 1997;349: 1599–1600.
14. Hossmann KA. Neuronal survival and revival during and after cerebral ischemia. *Am J Emerg Med*. 1994;1:191–197.
15. Hossmann KA. Viability thresholds and the penumbra of focal ischemia. *Ann Neurol*. 1994;36:557–565.
16. Astrup J, Symon L, Siesjö BK. Thresholds in cerebral ischemia: the ischemic penumbra. *Stroke*. 1981;12:723–725.
17. Symon L, Branston NM, Strong AJ, Hope TD. The concepts of thresholds of ischaemia in relation to brain structure and function. *J Clin Pathol*. 1977;30(suppl):149–154.
18. Heiss WD. Ischemic penumbra: evidence from functional imaging in man. *J Cereb Blood Flow Metab*. 2000;20:1276–1293.
19. Kluytmans M, van Everdingen KJ, Kappelle LJ, Ramos LM, Viergever MA, van der Grond J. Prognostic value of perfusion- and diffusion-weighted MR imaging in first 3 days of stroke. *Eur Radiol*. 2000;10: 1434–1441.
20. Moseley ME, Kucharczyk J, Mintorovitch J, Cohen Y, Kurhanewicz J, Derugin N, Asgari H, Norman D. Diffusion-weighted MR imaging of acute stroke: correlation with T2-weighted and magnetic susceptibility enhanced MR imaging in cats. *AJNR Am J Neuroradiol*. 1990;11: 423–429.
21. Moseley ME, Cohen Y, Mintorovitch J, Chileuitt L, Shimizu H, Kucharczyk J, Wendland MF, Weinstein PR. Early detection of regional cerebral ischemia in cats: comparison of diffusion and T2-weighted MRI and spectroscopy. *Magn Reson Med*. 1990;210:155–162.
22. Gonzalez RG, Schaefer PW, Buonanno FS, Schwamm LH, Budzik RF, Rordorf G, Wang B, Sorensen AG, Koroshetz WJ. Diffusion-weighted MR imaging: diagnostic accuracy in patients imaged within 6 hours of stroke symptom onset. *Radiology*. 1999;210:155–162.
23. Warach S, Chien D, Li W, Ronthal M, Edelman RR. Fast magnetic resonance diffusion-weighted imaging of acute human stroke. *Neurology*. 1992;42:1717–1723.
24. Warach S, Gaa J, Siewert B, Wielopolski P, Edelman R. Acute human stroke studied by whole brain echo planar diffusion-weighted magnetic resonance imaging. *Ann Neurol*. 1995;37:231–241.
25. Baird A, Warach S. Magnetic resonance imaging of acute stroke. *J Cereb Blood Flow Metab*. 1998;18:41–47.
26. Busza AL, Allen KL, King MD, van Bruggen N, Williams SR, Gadian DG. Diffusion-weighted imaging studies of cerebral ischemia in gerbils: potential relevance to energy failure. *Stroke*. 1992;10:1602–1612.
27. Warach S, Li W, Ronthal M, Edelman R. Acute cerebral ischemia: evaluation with dynamic contrast-enhanced MR imaging and MR angiography. *Radiology*. 1992;182:41–47.
28. Sorensen AG, Buonanno FS, Gonzalez RG, Schwamm LH, Lev MH, Huang-Hellinger FR, Reese TG, Weisskoff RM, Davis TL, Suwanwela N, Can U, Moreira JA, Copen WA, Look RB, Finklestein SP, Rosen BR, Koroshetz WJ. Hyperacute stroke: evaluation with combined multisection diffusion-weighted and hemodynamically weighted echo-planar MR imaging. *Radiology*. 1996;199:391–401.
29. Baird AE, Benfield A, Schlaug G, Siewert B, Lovblad KO, Edelman RR, Warach S. Enlargement of human cerebral ischemic lesion volumes measured by diffusion-weighted magnetic resonance imaging. *Ann Neurol*. 1997;41:581–589.
30. Barber PA, Darby DG, Desmond PM, Yang Q, Gerraty RP, Jolley D, Donnan GA, Tress BM, Davis SM. Prediction of stroke outcome with echoplanar perfusion- and diffusion-weighted MRI. *Neurology*. 1998;51: 418–426.
31. Rordorf G, Koroshetz WJ, Copen WA, Cramer SC, Schaefer PW, Budzik RF Jr, Schwamm LH, Buonanno F, Sorensen AG, Gonzalez G. Regional ischemia and ischemic injury in patients with acute middle cerebral artery stroke as defined by early diffusion-weighted and perfusion-weighted MRI. *Stroke*. 1998;29:939–943.
32. Lövblad KO, Baird AE, Schlaug G, Benfield A, Siewert B, Voetsch B, Connor A, Burzynski C, Edelman RR, Warach S. Ischemic lesion volumes in acute stroke by diffusion-weighted magnetic resonance imaging correlate with clinical outcome. *Ann Neurol*. 1997;42:164–170.
33. van Everdingen KJ, van der Grond J, Kappelle LJ, Ramos LM, Mali WP. Diffusion-weighted magnetic resonance imaging in acute stroke. *Stroke*. 1998;29:1783–1790.
34. Wintermark M, Maeder P, Thiran J-Ph, Schnyder P, Meuli R. Simultaneous measurements of regional cerebral blood flows by perfusion-CT and stable xenon-CT: a validation study. *AJNR Am J Neuroradiol*. 2001; 22:905–914.
35. Wintermark M, Reichhart M, Thiran J-P, Maeder P, Schnyder P, Bogousslavsky J, Meuli R. Prognostic accuracy of cerebral blood flow measurement by perfusion computed tomography, at the time of emergency room admission, in acute stroke patients. *Ann Neurol*. 2002;51:417-432.
36. Wintermark M, Maeder P, Verdun FR, Thiran JP, Valley JF, Schnyder P, Meuli R. Using 80 kVp versus 120 kVp in perfusion CT measurement of regional cerebral blood flows. *AJNR Am J Neuroradiol*. 2000;21: 1881–1884.

37. Wintermark M, Maeder P, Thiran J-Ph, Schnyder P, Meuli R. Quantitative assessment of regional cerebral blood flows by perfusion CT studies at low injection rates: a critical review of the underlying theoretical models. *Eur Radiol*. 2001;11:1220–1230.
38. Axel L. Cerebral blood flow determination by rapid-sequence computed tomography. *Radiology*. 1980;137:679–686.
39. Axel L. A method of calculating brain blood flow with a CT dynamic scanner. *Adv Neurol*. 1981;30:67–71.
40. Axel L. Tissue mean transit time from dynamic computed tomography by a simple deconvolution technique. *Invest Radiol*. 1983;18:94–99.
41. Ladurner G, Zilkha E, Iliff LD, du Boulay GH, Marshall J. Measurement of regional cerebral blood volume by computerized axial tomography. *J Neurol Neurosurg Psychiatry*. 1976;39:152–155.
42. Zilkha E, Ladurner G, Iliff LD, du Boulay GH, Marshall J. Computer subtraction in regional cerebral blood-size measurements using the EMI-scanner. *Br J Radiol*. 1976;49:330–334.
43. Ladurner G, Zikha E, Sager WD, Iliff LD, Lechner H, du Boulay GH. Measurement of regional cerebral blood volume using the EMI 1010 scanner. *Br J Radiol*. 1979;52:371–374.
44. Harper AM. Autoregulation of cerebral blood flow: influence of the arterial blood pressure on the blood flow through the cerebral cortex. *J Neurol Neurosurg Psychiatry*. 1966;29:398–403.
45. Mayer TE, Hamann GF, Baranczyk J, Rosengarten B, Klotz E, Wiesmann M, Missler U, Schulte-Altedorneburg G, Brueckmann HJ. Dynamic CT perfusion imaging of acute stroke. *AJNR Am J Neuroradiol*. 2000;21:1441–1449.
46. Hunter GJ, Hamberg LM, Ponzo JA, Huang-Hellinger FR, Morris PP, Rabinov J, Farkas J, Lev MH, Schaefer PW, Ogilvy CS, Schwamm L, Buonanno FS, Koroshetz WJ, Wolf GL, Gonzalez RG. Assessment of cerebral perfusion and arterial anatomy in hyperacute stroke with three-dimensional functional CT: early clinical results. *AJNR Am J Neuroradiol*. 1998;19:29–37.
47. Lee KH, Cho SJ, Byun HS, Na DG, Choi NC, Lee SJ, Jin IS, Lee TG, Chung CS. Triphasic perfusion computed tomography in acute middle cerebral artery stroke: a correlation with angiographic findings. *Arch Neurol*. 2000;57:990–999.
48. Sorensen AG, Reimer P. *Cerebral MR Perfusion Imaging: Principles and Current Applications*. New York, NY: Thieme Verlag; 2000.
49. Boxerman JL, Hamberg LM, Rosen BR, Weisskoff RM. MR contrast due to intravascular magnetic susceptibility perturbations. *Magn Reson Med*. 1995;34:555–566.
50. Weisskoff R, Zuo C, Boxerman J, Rosen B. Microscopic susceptibility variation and transverse relaxation: theory and experiment. *Magn Reson Med*. 1994;31:610.
51. Koenig M, Klotz E, Luka B, Venderink DJ, Spittler JF, Heuser L. Perfusion CT of the brain: diagnostic approach for early detection of ischemic stroke. *Radiology*. 1998;209:85–93.
52. Mayer TE, Hamann GF, Baranczyk J, Rosengarten B, Klotz E, Wiesmann M, Missler U, Schulte-Altedorneburg G, Brueckmann HJ. Dynamic CT perfusion imaging of acute stroke. *AJNR Am J Neuroradiol*. 2000;21:1441–1449.
53. Eastwood JD, Lev MH, Azhari T, Lee TY, Barboriak DP, Delong DM, Fitzek C, Herzau M, Wintermark M, Meuli R, Brazier D, Provenzale JM. CT perfusion scanning with deconvolution analysis: pilot study in patients with acute middle cerebral artery stroke. *Radiology*. 2002;222:227–236.
54. Grant PE, He J, Wu O, Schaefer PW, Schwamm LH, Budzik RF, Sorensen AG, Koroshetz WJ, Gonzalez RG. Frequency and clinical context of decreased apparent diffusion coefficient reversal in the human brain. *Radiology*. 2001;221:43–50.
55. Yamada K, Wu O, Gonzalez RG, Bakker D, Ostergaard L, Copen WA, Weisskoff RM, Rosen BR, Yagi K, Nishimura T, Sorensen AG. Magnetic resonance perfusion-weighted imaging of acute cerebral infarction: effect of the calculation methods and underlying vasculopathy. *Stroke*. 2002;33:87–94.
56. Doerfler A, Engelhorn T, von Kummer R, Weber J, Knauth M, Heiland S, Sartor K, Forsting M. Are iodinated contrast agents detrimental in acute cerebral ischemia? An experimental study in rats. *Radiology*. 1998;206:211–217.